



Effect of extra-framework cesium on the deoxygenation of methylester over CsNaX zeolites

Tanate Danuthai^{a,1}, Tawan Sooknoi^b, Siriporn Jongpatiwut^c, Thirasak Rirksomboon^c, Somchai Osuwan^c, Daniel E. Resasco^{a,*}

^a School of Chemical, Biological and Materials Engineering, University of Oklahoma, Norman, OK 73019, USA

^b Department of Chemistry, Faculty of Science, King Mongkut's Institute of Technology Ladkrabang, Bangkok 10520, Thailand

^c Center for Petroleum, Petrochemicals, and Advanced Materials, The Petroleum and Petrochemical College, Chulalongkorn University, Patumwan, Bangkok 10330, Thailand

ARTICLE INFO

Article history:

Received 26 May 2011

Received in revised form

18 September 2011

Accepted 25 September 2011

Available online 1 October 2011

Keywords:

Deoxygenation

Decarbonylation

Methylesters

Biofuels

CsNaX

Basicity

Cesium

ABSTRACT

The deoxygenation of methyl octanoate has been investigated over Cs-containing NaX zeolite catalysts at atmospheric pressure with He carrier gas and methanol as a co-feed. By varying the preparation procedures, different amounts of extra-framework Cs were left on the catalyst. The presence of extra-framework Cs affects the acid–basic characteristics of the catalysts and consequently their activity, stability, and particularly the product selectivity. That is, when the amount of extra-framework Cs increases, the corresponding increase in basicity enhances decarbonylation activity as well as catalyst stability. In this case, the deoxygenation of methyl octanoate on CsNaX catalysts was found to yield heptenes and hexenes as main products via surface decomposition of octanoate-like species. When the amount of extra-framework Cs was reduced, the hexene yield readily increased. The enhancement in hexene production can be ascribed to both, a decreased basicity that reduces decarbonylation and to a greater space available within the zeolite cavity for formation of a rather bulky cyclic-like intermediate that leads to hexene. In addition, weakly acidic sites, generated after the excess Cs was removed, resulted in relatively higher yield of inner-olefin product. When Cs was not present in the catalyst (i.e., NaX), other products such as aromatics and coupling compounds were observed. These compounds are less desirable for transportation fuel applications.

© 2011 Elsevier B.V. All rights reserved.

1. Introduction

Fatty acid methyl esters (FAMES), produced from the transesterification of vegetable oil or animal fats with alcohol, have received considerable attention to use as biodiesel [1–3]. However, while FAMES have high cetane number, the thermal and chemical instability caused by the presence of oxygen in the molecules, is a major technical concern [4,5]. Upgrading of biodiesel to eliminate oxygen has been extensively studied. In most cases, the process involves the use of hydrotreating or hydrogenation catalysts, such as metal sulfides and supported noble metals, under high hydrogen pressure [6–8]. Some recent studies have focused on alternative catalysts, especially zeolites [9–11], to conduct the upgrading under milder operating conditions. We have recently reported that the deoxygenation of methyl octanoate can be effectively accomplished over

a Cs-exchanged zeolite with low Si/Al ratio (CsNaX) under atmospheric pressure and in the absence of hydrogen [12]. It has been demonstrated that the combination of the highly active basic properties of the CsNaX zeolite catalyst, with methanol as a co-fed reactant, appears very effective for the conversion of methyl ester. We proposed that the highly polar environment of the zeolite micropore plays an essential role in the adsorption and decomposition of the adsorbed species.

In the present contribution, we have explored the role of the extra-framework Cs cations in zeolite X. We have investigated the conversion of the methyl octanoate as a FAME model compound over Cs-exchanged NaX zeolite catalysts, containing varying amounts of extra-framework Cs. For comparison, the catalytic activities of Cs/SiO₂, CsUSY, CsNaY catalysts were also investigated.

2. Experimental

2.1. Catalyst preparation and characterization

Three commercial X and Y zeolites were used as catalysts. The NaX (UOP type 13X, Si/Al = 1.2) was obtained from Fluka. The H-USY (CBV 720, Si/Al = 16) and NaY (CBV 100, Si/Al = 2.4) were purchased

* Corresponding author. Tel.: +1 405 325 4370; fax: +1 405 325 5813.

E-mail address: resasco@ou.edu (D.E. Resasco).

¹ Current address: Institute of Chemical and Engineering Sciences, Agency for Science, Technology, and Research (A*STAR), 1 Pesek Rd., Jurong Island, Singapore 627833, Singapore.

from Zeolyst. All as-received materials were calcined at 723 K. The Cs-containing zeolite (CsNaX) was prepared by ion exchange of the zeolite with a 0.1 M CsNO₃ solution at 353 K for 24 h. The resulting solid material was filtered and left to dry at 353 K overnight. The sample was then calcined at 723 K for 2 h in a flow of dry air. This sample is referred to as CsNaX20, while those after washing 4 and 7 times, are referred to as CsNaX5 and CsNaX2, respectively, in which the suffix numbers represent the extra-framework Cs content, calculated based on the measured amounts of Na, Al, and Cs. To compare with the microporous catalyst, a 20 wt% Cs/SiO₂ catalyst was prepared by conventional incipient wetness impregnation using cesium nitrate solution as impregnating precursor. The elemental composition of the catalysts was analyzed by inductively coupled plasma optical emission spectroscopy (ICP-OES). The catalyst surface areas were determined by nitrogen adsorption at 77 K using a Micromeritics ASAP 2000 apparatus. X-ray diffraction (XRD, Bruker AXS D8Discover) was used to corroborate the zeolite structure. The hydrogen uptake of the Cs-containing catalysts was measured by temperature programmed reduction (TPR).

2.2. FTIR of the adsorbed acetonitrile

The basic strength of the Cs-containing NaX zeolite catalysts was determined by FTIR using acetonitrile as a probe molecule, following an established method [13]. Infrared spectroscopic measurements of the adsorbed acetonitrile were recorded on a Bruker Equinox 55 Spectrometer. Self-supported wafer samples were prepared and placed in a gas-tight cell. Initially, the samples were pretreated in a flow of 2% O₂/He at 723 K for 2 h. After pretreatment, they were cooled to room temperature in flow of He. Acetonitrile was then injected (10 μl) to the sample cell in flow of He, which was maintained for 5 h to purge the excess acetonitrile. At this point, a spectrum was taken and compared to that obtained in pure He.

2.3. Temperature programmed desorption (TPD) of the isopropylamine (IPA)

The catalyst acidity was tested by the amine TPD technique developed by Gorte and co-workers [14]. First, a 50 mg sample was pretreated at 723 K in flow of 2% O₂/He for 1 h. After pretreatment, the sample was cooled in He to room temperature and then consecutive pulses (10 μl) of isopropylamine (IPA) were injected into the sample until saturation was achieved, as indicated by a constant $m/z = 44$ signal in the MS. After removing the excess of IPA by flowing He for 3 h, the sample was linearly heated to 973 K at a heating rate of 10 K/min. Masses (m/z) of 44, 41, and 17 were monitored to determine the evolution of desorbing isopropylamine, propylene, and ammonia, respectively. The amount of desorbed IPA was calibrated with 50 μl pulses of 2% propylene in He ($m/z = 41$).

2.4. Temperature programmed oxidation (TPO)

Temperature programmed oxidation (TPO) was used to investigate the nature and quantify the amount of coke deposited on the spent catalysts. In each TPO, a 30 mg sample was packed in a 1/4 in. quartz tube reactor, the temperature was ramped to 1173 K with a heating rate of 10 K/min, and the TPO profiles were recorded under a flow of 2% O₂/He. The CO₂ produced by the oxidation of the coke deposits was further converted to methane over a methanation catalyst (15% Ni/Al₂O₃) in the presence of hydrogen at 673 K. The methane produced was then analyzed online by an FID detector. The amount of coke oxidized was calibrated using 100 μl pulses of pure CO₂ injected into the same system.

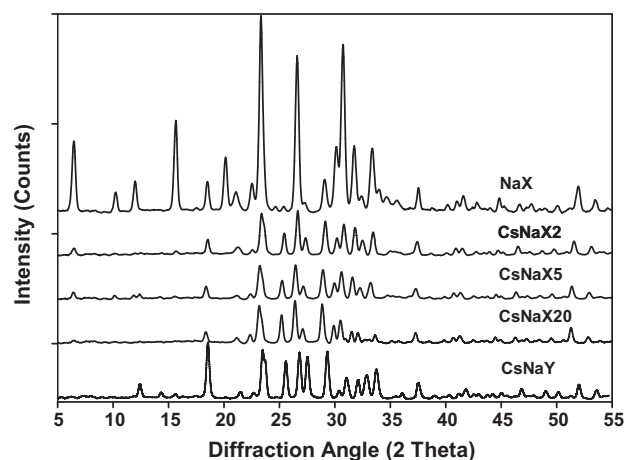


Fig. 1. XRD profiles of the NaX, CsNaX, and CsNaY catalysts.

2.5. Catalytic activity measurements for the deoxygenation of methyl octanoate

The deoxygenation of methyl octanoate was carried out at atmospheric pressure, in a fixed-bed flow reactor made with a 1/4 in. quartz tube. Prior to the reaction, the catalyst samples were pretreated *in situ* under a flow of 2% O₂/He at 723 K for 2 h. Then, the catalyst bed was cooled to the reaction temperature (698 K) under a flow of He (25 ml/min). The reactant feed of 10 wt% methyl octanoate in a methanol solvent was introduced into the reactor using a syringe pump via a heated vaporization port. Unreacted feed and products were quantified using an online GC-FID equipped with a capillary HP-5 column, using a temperature program to optimize product separation.

3. Results and discussion

3.1. Characterization of the fresh catalysts

The XRD patterns of the Cs-exchanged NaX catalysts (Fig. 1) exhibited the same reflections as that of the parent faujasite, which demonstrates that the original structure of the NaX is retained after the ion exchange and washing treatments. The position of the reflections remains almost unchanged. The zeolite unit cells have been calculated for the different samples by using the reflections from (440), (533), and (642) planes [15]. The results are as follows: NaX (24.7 ± 0.2 Å); CsNaX2 (24.9 ± 0.1 Å); CsNaX5 (24.8 ± 0.2 Å); CsNaX20 (24.9 ± 0.2 Å), in good agreement with published data [15–17]. That is, while Cs incorporation results in a slight increase in unit cell size, higher Cs loadings do not cause further increase since most of these excess Cs is extra-framework. On the other hand, the peak intensity decreases for the Cs-exchanged samples. As suggested in previous studies [18,19], this decrease in intensity can be ascribed to the higher extent of X-ray absorption of the Cs⁺ cations incorporated in the zeolite. As expected, similar behavior, i.e., same reflections with reduced intensity were observed for the Cs-exchanged NaY and USY zeolites (not shown). This observation is consistent with previous reports [20,21], which indicated that all Cs-exchanged Y zeolites keep the same crystalline phase and framework structure after the various exchange and washing procedures.

The ICP-OES elemental analysis indicated that, based on the amount of Na removed, all catalysts reached about the same extent of ion exchange (approximately 35%). However, by comparing the total content of Cs incorporated to the amounts of Na and Al

Table 1
Physical data of the NaX, CsNaX, and CsNaY catalysts.

Catalyst	Surface area (m ² /g)	Si/Al	Unit cell composition ^a					Excess Cs per unit cell
			Al	Si	O	Na	Cs	
NaX	695	1.2	91.5	100.5	384.0	91.5	0.0	0.0
CsNaX2	522	1.1	88.0	104.0	384.0	58.7	29.3	2.2
CsNaX5	439	1.2	91.3	100.7	384.0	59.5	31.8	4.9
CsNaX20	367	1.2	86.9	105.1	384.0	54.4	32.5	19.8
CsNaY	378	2.4	57.2	134.8	384.0	17.6	39.7	17.3

^a Based on standard faujasite unit cell ($M_n^+(Al_nSi_{192-n}O_{386})$) with $n = 87-96$.

remaining in the zeolite it becomes immediately obvious that a significant fraction of the Cs incorporated must not be replacing Na cations in the framework, but rather occluded as extra-framework Cs (Table 1). It observed that these extra-framework Cs species lead to a sizeable drop in BET surface area and pore volume, as compared to those of the parent NaX zeolite. However, a partial recovery of the original surface area is observed when a significant fraction of the extra-framework Cs species is eliminated by washing (e.g., samples CsNaX5 and CsNaX2).

It was found that the hydrogen consumption observed by TPR for each catalyst correlates well with the amount of extra-framework Cs calculated from the ICP analysis. That is, while significant hydrogen uptake was observed for the CsNaX20 zeolite, no uptake was observed for the plain NaX sample (Fig. 2). Moreover, a significantly lower hydrogen uptake was found after the washing treatment, as observed for the samples CsNaX5 and CsNaX2. We explain this contrasting behavior of the different samples in terms of the different amounts of extra-framework Cs, which can form clusters of different oxidized species (e.g., cesium oxide, cesium peroxide, cesium superoxide, cesium carbonate) during the calcination step in flow of air. Therefore, the hydrogen uptake observed by TPR can be taken as a good measure of the amount of extra-framework Cs species [22,23]. Accordingly, the decrease in hydrogen uptake observed on samples CsNaX5 and CsNaX2 is another indication that the washing treatment causes removal of extra-framework Cs. In good agreement with this conclusion, the TPR of a CsNaY sample was similar to that of the CsNaX20 sample. The reduction peak appears at about the same temperature but the hydrogen uptake working with the CsNaY sample was significantly lower than that with CsNaX20, which of course can be explained by a lower extent of extra-framework Cs in the CsNaY sample.

3.2. Acid–base characterization

To characterize the basicity of the catalysts we used FTIR of adsorbed acetonitrile. As proposed in previous work [13,24], the position of the band corresponding to the stretching of the C≡N group of acetonitrile can be used as a relative measure of catalyst basic strength. That is, as the basicity increases the vibrational frequency of the C≡N group in the adsorbed acetonitrile decreases. A stronger basic site results in a higher electron density in the adsorbate, which in turn lengthens the C≡N bond, resulting in a decrease in vibrational frequency. As shown in Fig. 3, the absorption band for the stretching mode of C≡N in acetonitrile adsorbed on NaX appears at 2257 cm⁻¹, which is slightly higher than that for acetonitrile in the gas phase (2254 cm⁻¹) [25]. By contrast, when Cs is present on the catalyst, a significant shift to lower frequencies is observed. The shift seems to be largest on the sample with highest extra-framework Cs content, and becomes less noticeable after the washing treatments. That is, the basic strengths of the catalysts follows the sequence CsNaX20 > CsNaX5 > CsNaX2 > NaX. While for some of them the differences are small, it has been shown that differences as small as 1 cm⁻¹ correlate with significant differences in basicity [13].

Consistent with this trend, the TPD of adsorbed IPA gives evidence for residual acidity only on the catalysts with low basicity. As shown in Fig. 4, desorption at about 450 K is indicative of rather weak (physical) IPA adsorption, while desorption at higher temperature (~630 K) may indicate the presence of acid sites. A slight increase in the amount of these more-strongly adsorbed IPA was observed as the density of extra-framework Cs species decreased. That is, when the extra-framework Cs is removed by the washing treatment, acid sites of moderate strength are formed. As expected, a significantly larger amount of more-strongly adsorbed IPA was

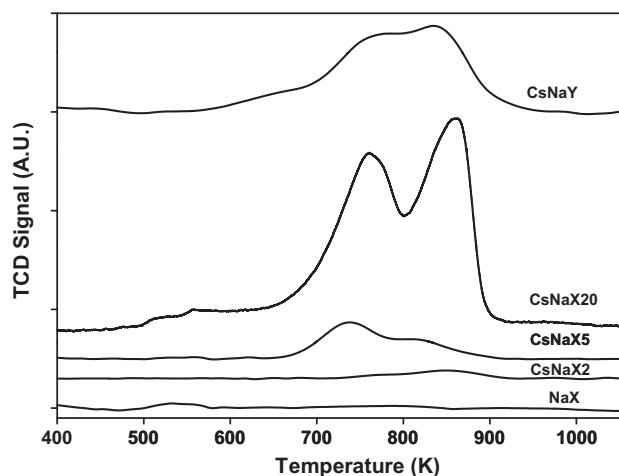


Fig. 2. TPR profiles of the NaX, CsNaX, and CsNaY catalysts, all treated in air at 723 K before starting the TPR.

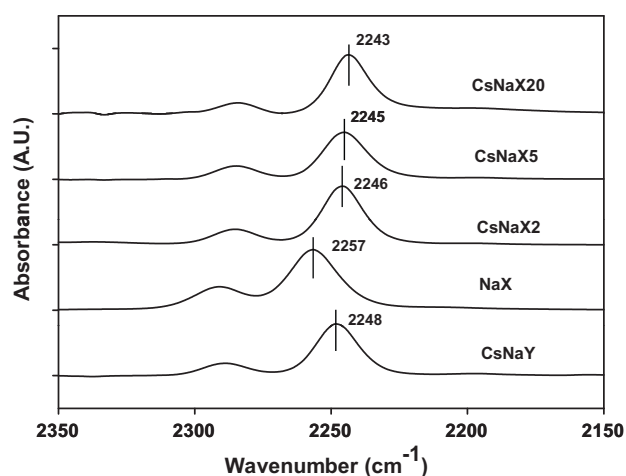


Fig. 3. FTIR spectra of adsorbed acetonitrile over the NaX, CsNaX, and CsNaY catalysts.

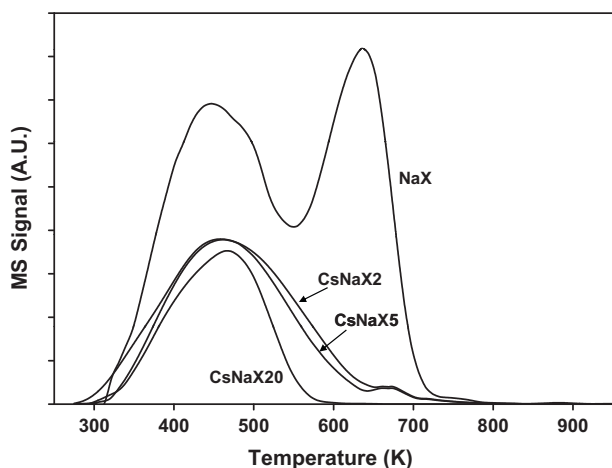


Fig. 4. Evolution of $m/z=44$ during the TPD of isopropylamine over the NaX and CsNaX catalysts.

observed on the Cs-free NaX zeolite (of moderate acidity). However, it must be noted that even in this latter case, the strength of the acidity is much lower than that of a typical H-form zeolite, such as H-ZSM-5.

3.3. Reactions of methyl octanoate

3.3.1. CsNaX catalysts

The effect of the extra-framework Cs on the activity and stability of CsNaX zeolite catalysts was investigated at 698 K and atmospheric pressure using a gaseous feed of 10 wt% methyl octanoate in methanol vaporized in a He carrier gas. The overall conversion obtained over the various catalysts containing different amounts of the extra-framework Cs is compared in Fig. 5 as a function of time-on-stream. It is clear that the NaX catalyst (free of Cs) exhibits a high initial activity, but it rapidly deactivates in the presence of the feed. By contrast, a relatively lower activity but much better stability as a function of time-on-stream is clearly evident for the CsNaX20 catalyst, which has the largest amount of the extra-framework Cs. The activity and stability of the CsNaX5 and CsNaX2 catalysts, containing relatively lower amounts of the extra-framework Cs, fall between those of CsNaX20 and NaX catalysts. This clear trend demonstrates that the presence of the extra-framework Cs species enhances catalyst stability.

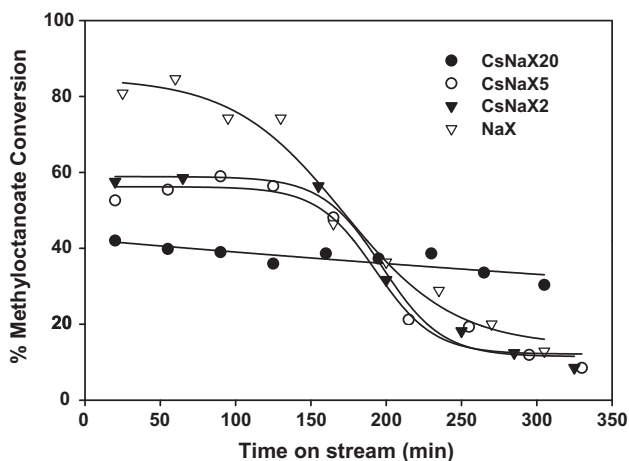


Fig. 5. Conversion of 10 wt% methyl octanoate in methanol over the CsNaX and NaX catalysts with various extra-framework cesium contents. Reaction conditions: 698 K, 1 atm, $W/F=198$ g h/mol, 25 ml/min of He.

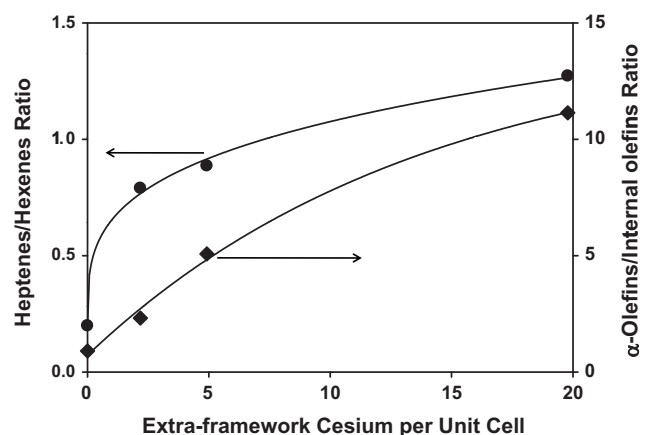


Fig. 6. Heptenes/hexenes ratio and α -olefins/internal olefins ratio as a function of extra-framework cesium per unit cell.

As shown in our previous study [12], the adsorption of methanol on the CsNaX catalyst leads to the formation of surface formate species and hydrogen [26]. In that study we proposed that these surface formate species suppress the formation of high-molecular weight condensation compounds, while the surface hydrogen helps keeping the catalyst clean. Accordingly, the stability improvement observed here with increasing extra-framework Cs could be explained by an enhanced methanol adsorption due to the high basicity caused by the presence of excess Cs [27]. By contrast, in the absence of Cs species (NaX), the surface reaction of methanol may lead to dimethyl ether, instead of hydrogen, as previously reported [28]. That is, much less surface hydrogen and surface formate species should be expected on this catalyst, which is consistent with the observed deactivation rate.

The presence of the extra-framework Cs not only improves stability and lowers the initial conversion, but also affects the product distribution. Table 2 summarizes the product distribution from the reaction of methyl octanoate after 20 and 370 min on stream. While heptenes and hexenes are the main products for all the catalysts investigated, the ratio between these two major products is seen to vary significantly among the various catalysts. As shown in Fig. 6, when plotting the heptenes/hexenes ratio as a function of the extra-framework Cs per unit cell a clear trend is observed. We have recently proposed that while heptenes clearly arise from decarbonylation of the methyl octanoate feed, hexenes may be formed by decetalization (or deacetalation, i.e., elimination of CH_3CHO) [12].

We proposed that the decarbonylation of the methyl octanoate can take place through primary decomposition at the methoxyl group of the methylester, which results in an octanoate-like species that plays the role of an intermediate that further decomposes to either heptenes or hexenes as final products [12]. As illustrated in Scheme 1 below, the formation of heptenes can proceed through β -hydrogen elimination with subsequent decomposition on a basic site [29]. By contrast, one can speculate that the formation of hexenes would involve a cyclic-like intermediate that may require an acid–base pair-interaction and a relatively large space to accommodate this intermediate. Accordingly, catalysts with less restrictive pore sizes, reduced basicity, and weak acidity could lead to the production of hexene. In fact, the observed increased surface area and weak acidity generated by elimination of the large polarizable Cs cations indicate that the washed samples (CsNaX5 and CsNaX2) could be such catalysts that facilitate the formation of the cyclic-like intermediate. Therefore, it is more likely that the adsorbed octanoate-like intermediate might undergo decomposition via the

Table 2
Product distribution from the reaction of 10 wt% methyl octanoate in methanol over the CsNaX and NaX catalysts.

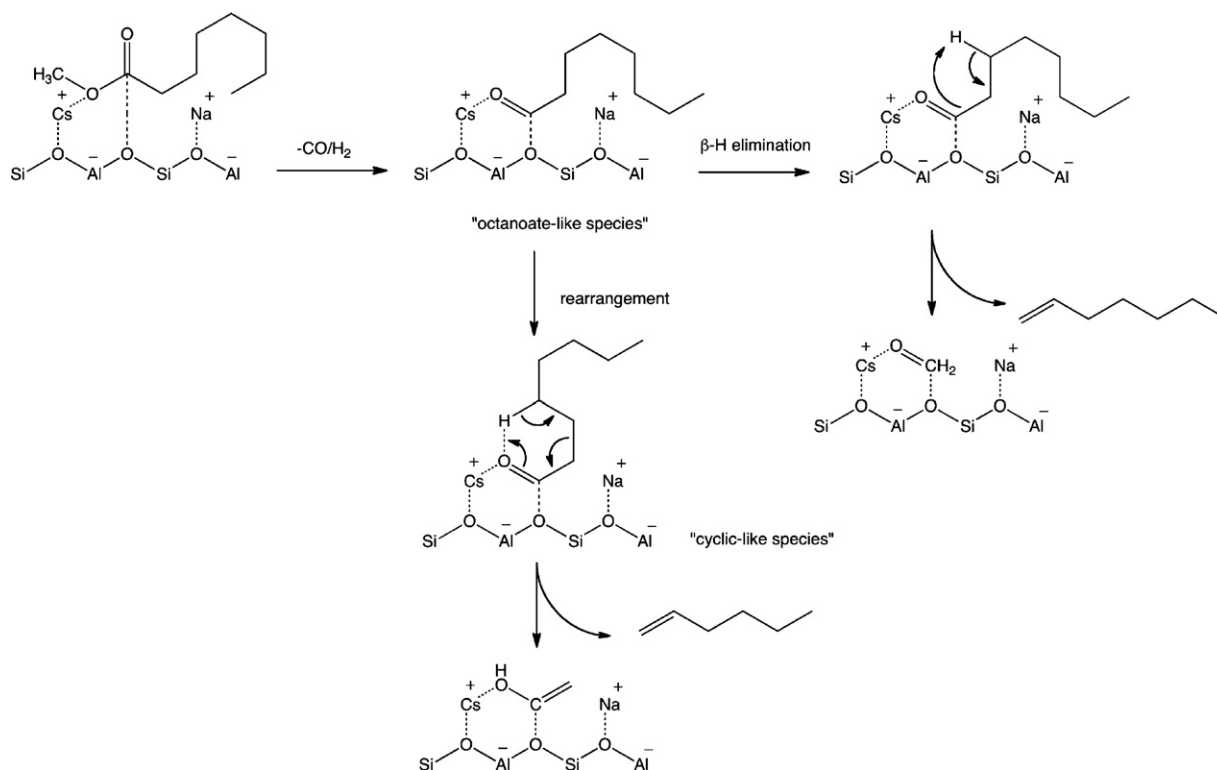
TOS (min)	Catalysts							
	CsNaX20		CsNaX5		CsNaX2		NaX	
	20	300	20	300	20	300	20	300
Conversion	43.0	29.0	52.5	19.2	55.6	12.4	80.8	12.9
C7/C6 Ratio	1.3	2.2	1.0	1.5	0.8	1.0	0.8	0.9
Yield (wt%)								
a-Hexenes	9.8	4.9	11.8	3.2	6.6	2.1	3.7	3.3
Hexenes	1.6	0.9	4.0	1.3	10.2	1.0	10.9	1.6
n-Hexane	0.8	0.2	1.4	0.3	5.6	0.3	5.2	0.4
a-Heptenes	13.7	12.1	12.5	5.9	10.9	2.5	2.4	4.5
Heptenes	0.8	0.3	1.5	0.4	2.5	0.4	0.5	0.0
n-Heptane	1.6	0.7	2.9	0.8	3.5	0.6	13.0	0.3
Octenes	2.7	2.8	2.8	1.8	2.0	0.8	5.6	0.8
n-Octane	0.7	0.3	0.9	0.3	0.7	0.1	0.4	0.1
Oxygenates								
-Octanal	3.1	2.0	6.2	0.8	6.2	1.1	4.4	0.6
-Octanoic acid	1.6	0.6	2.2	1.2	1.7	0.6	2.8	0.2
-Oxygenates	1.0	0.5	1.1	0.2	1.0	0.4	15.7	1.0
Condensation products								
-Pentadecene	0.4	0.0	0.7	0.0	1.4	0.0	1.4	0.1
-Pentadecanone	4.6	3.3	3.9	2.7	2.8	2.2	0.0	0.0
-Coupling ester	0.6	0.4	0.6	0.3	0.5	0.4	0.0	0.0
Aromatics	0.0	0.0	0.0	0.0	0.0	0.0	14.8	0.1

proposed intermediate, producing more hexene, rather than heptene via β -hydrogen elimination.

In line with this hypothesis, the NaX catalyst (free of Cs and containing the highest acidity in the series) yields much higher amounts of hexenes and consequently the lowest heptenes/hexenes ratio (see Fig. 6). In addition, some multi-substituted aromatic products were obtained on the NaX catalyst. This type of products arises from acid-catalyzed reactions (aromatization, alkylation, and isomerization), which is again consistent with the presence of acid sites in NaX. Our previous contributions [30–32] demonstrated that the aromatization of the oxygenate compounds

(e.g., methyl ester and aldehydes) readily occurs over acid zeolites, such as HZSM-5. The reaction can proceed either through the direct ring closure of the ester by the activation of the H atom bonded to the C in the α position relative to the carbonyl group or via oligomerization, followed by cyclization, of olefins from the short-chain hydrocarbon pool generated on the surface from cracking of the oxygenates. In the present case, since methanol is present in the feed, it can also act as a methylating agent over the acid sites, leading to the formation of multi-substituted aromatics [33–35].

In addition to heptenes and hexenes, the appearance of octenes in the products suggests that hydrogenation and dehydration can



Scheme 1. Reaction pathways.

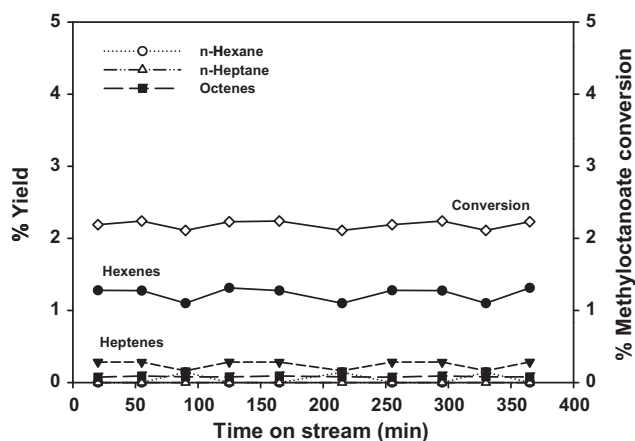


Fig. 7. Conversion and product distributions of 10wt% methyl octanoate in methanol over the Cs/SiO₂ catalyst. Reaction conditions: 698 K, 1 atm, W/F=198 g h/mol, 25 ml/min of He.

also occur over the cesium-exchanged zeolites. That is, if surface hydrogen from the decomposition of methanol can hydrogenate the adsorbed octanoate-like species, octanol could result, which can rapidly dehydrate and form octenes (see Scheme 1). However, the extent of this reaction is relatively low in comparison to that of decarbonylation of the octanoate-like species.

Moreover, the presence of alkanes (hexane, heptanes, and octane) in the product gives another evidence for the hydrogenation activity of CsNaX zeolite catalysts, most probably occurring via hydrogen transfer. Our previous study on the H-D exchange experiment demonstrated that hydrogen transfer takes place on the zeolite surface, enhanced by the highly polarizable environment within the restricted pores of the zeolite [36]. It was found that the yields of hexane and heptane increased with decreasing extra-framework Cs. As shown in Table 2, this decreasing Cs content results in an increase in pore volume and surface area. It must be noted that both, hexane and heptane, arise from their olefinic counterparts. Hence, it is important to analyze the variation of the alkane/alkene ratio for both, C7 and C6. In line with the heptenes/hexenes ratio in Fig. 6, the relative C7/C6 ratio increases with increasing extra-framework cesium species (Table 2).

Fig. 6 also includes another interesting trend in product distribution with the amount of extra-framework cesium per unit cell; this is the ratio of α - to internal olefins in the product. While α -olefins are directly obtained from the decarbonylation reaction [37,38], the internal olefins result from double-bond isomerization, which is typically catalyzed by acid sites [39]. Therefore, the increase in the α -olefins/internal olefins ratio with increasing extra-framework Cs content is consistent with the proposed change in the acid–base balance associated with the presence of Cs. That is, the fraction of α -olefins in the olefin product, the IR shifts of adsorbed acetonitrile, and the TPD of adsorbed IPA all indicate that the balance basicity-to-residual acidity of the series follows the sequence proposed above, i.e., CsNaX20 > CsNaX5 > CsNaX2 > NaX.

3.3.2. Cs/SiO₂, CsUSY, and CsNaY catalysts

To determine whether any occluded Cs species can have similar role in activity as the extra-framework Cs species present on the CsNaX catalysts, we conducted the methyl octanoate reaction on other Cs-containing catalysts under the same conditions as those used with CsNaX. Fig. 7 shows the conversion and the product distribution obtained over the Cs/SiO₂ catalyst. It is clearly seen that the activity of this catalyst (~2% conversion) is much lower than that of the CsNaX series (~40–55% conversion).

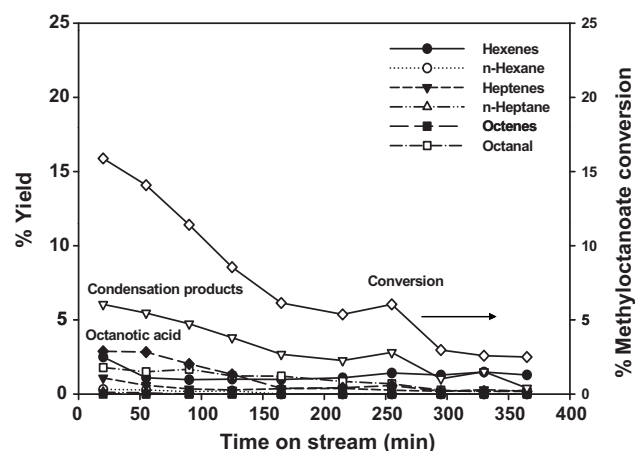


Fig. 8. Conversion and product distributions of 10wt% methyl octanoate in methanol over the CsUSY catalyst. Reaction conditions: 698 K, 1 atm, W/F=198 g h/mol, 25 ml/min of He.

In a second comparison, a high-silica zeolite (i.e., low number of sites and exchangeable cations) catalyst with extra-framework Cs species was investigated. As shown in Fig. 8, the activity of the high-silica CsUSY (Si/Al = 16) catalyst was relatively higher than that of Cs/SiO₂, but it rapidly deactivated and yielded undesired products. For instance, coupling products from the condensation reaction, namely pentadecanone and coupling ester, were obtained as major products, together with octanoic acid. The more desirable (from biofuels prospective) decarbonylation products, such as hexenes and heptenes, were only produced in small amounts. Therefore, it can be concluded that extra-framework Cs by itself does not guarantee the enhanced decarbonylation or hydrogenation activity observed on CsNaX catalysts.

In the third comparison, a CsNaY (Si/Al = 2) catalyst was used. It is well known that the NaY zeolite has a similar structure as that of NaX zeolite. However, the Si/Al ratio is almost twice as high, which significantly changes the acid–base characteristics [40]. In fact, the FTIR spectra of the acetonitrile adsorbed on CsNaY (Fig. 3) shows that the absorption band of the C≡N group appears at 2248 cm⁻¹, which is higher than that on CsNaX20 (2243 cm⁻¹). This suggests that the unwashed CsNaY sample has a lower basic strength than the CsNaX20. This may be attributed to the lower amount of basic framework oxygen of the CsNaY catalyst, leading to the reduction in the electron density in the C≡N bond of the adsorbed acetonitrile.

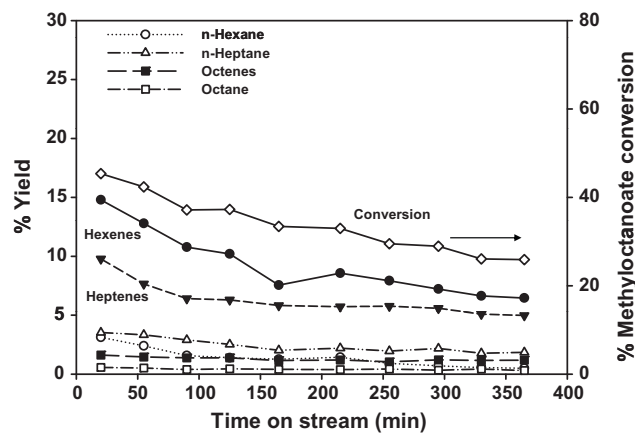


Fig. 9. Conversion and product distributions of 10wt% methyl octanoate in methanol over the CsNaY catalyst. Reaction conditions: 698 K, 1 atm, W/F=198 g h/mol, 25 ml/min of He.

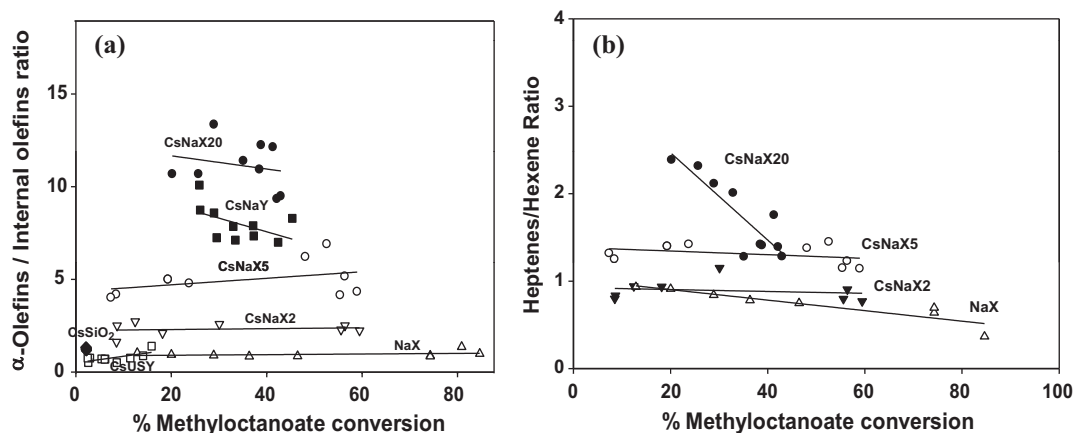


Fig. 10. α -Olefins/internal olefins (a) and Heptenes/Hexenes (b) ratios as a function of methyl octanoate conversion over various catalysts.

The observed product distribution on this catalyst is significantly different from that on the unwashed CsNaX. The CsNaY catalyst yielded hexenes as the main products, followed by heptenes, as illustrated in Fig. 9. As mentioned above, we propose that the formation of hexenes arises from the cyclic-intermediates on the catalyst surface. This step may be favored on NaX and CsNaY due to two different reasons. The first one is a lower basicity on these catalysts compared to CsNaX. The second is a more open space inside the zeolite cavities. Both characteristics of NaX and CsNaY would allow the cyclic intermediate that produces hexene instead of direct decarbonylation of the octanoate-like species that produces heptenes. By contrast, on the CsNaX, both higher basicity and more geometric restrictions due to the large amount of Cs cations in the crystal, would restrict the formation of the cyclic-intermediate and favor decarbonylation.

As clearly shown in Fig. 10(a), the α -to-internal olefin ratio is clearly different among the various catalysts investigated. Over the entire conversion range, the catalysts with low basicity (i.e., CsUSY and Cs/SiO₂) exhibit a ratio that is much lower than those for the catalysts in the CsNaX series. The α -to-internal olefin ratio is in fact a good indicator of the decarbonylation-to-double-bond isomerization ratio. The former is catalyzed by basic sites while the latter is facilitated by the acid ones. Therefore, the weaker basicity of Cs/SiO₂, CsUSY, and CsNaY catalysts results in less decarbonylation and more isomerization. In parallel, the hexenes/heptenes ratio is shown in Fig. 10(b) to demonstrate that while this ratio is a weak function of conversion, it is a function of the extra-framework Cs for any given conversion. In agreement with Fig. 6, the heptenes/hexenes ratio increases in the direction NaX < NaX2 < NaX5 < NaX20.

3.4. Characterization of the spent catalysts

The coke deposits formed on the catalysts during reaction were quantified by TPO and the results shown in Fig. 11. On the Cs-containing zeolite catalysts, less than twice as much coke was deposited during the reaction of 10 wt% methyl octanoate, compared to that on the Cs-free NaX catalyst. The TPO profiles display two carbon oxidation peaks, one at a relatively lower temperature (~500 K) and another at higher temperature (~620 K). It is expected that the coke deposits on the CsNaX catalysts contain high-molecular-weight oxygenates rather than the typical polyaromatic coke, which normally oxidizes above 820 K.

In general, the catalysts with less extra-framework Cs produced somewhat larger amounts of coke, and the deposits were oxidized at higher oxidation temperature. This behavior was particularly obvious on the NaX catalyst (Cs-free) and is consistent with the

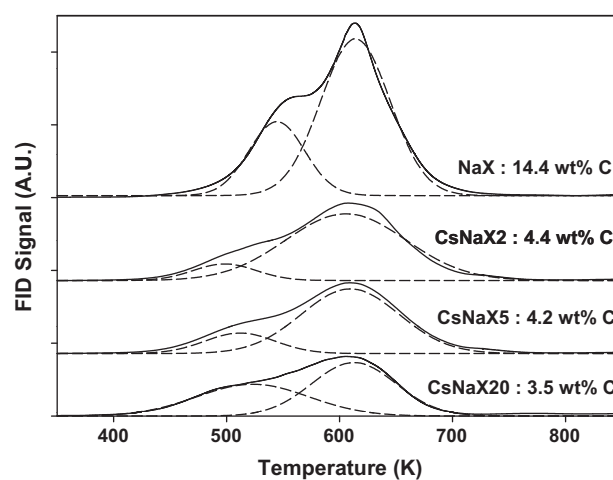


Fig. 11. TPO profiles of the spent NaX and CsNaX catalysts from the reaction of 10 wt% methyl octanoate in methanol.

higher acid/base ratio (see TPD of IPA) and the formation of the higher-molecular-weight compounds (namely pentadecenes, pentadecanone, and coupling esters) when the catalysts contain less extra-framework Cs (see Table 2).

4. Conclusions

Methyl octanoate, a model fatty acid methyl ester, can be effectively decarbonylated and deacetalized at atmospheric pressure and in the absence of added hydrogen over CsNaX zeolites, when using methanol as co-feed. The main products of these reactions are heptenes and hexenes, respectively. The extra-framework Cs plays a crucial role in determining the performance of the catalyst; a stronger basicity is generated by the presence of extra-framework Cs and this basicity determines the product selectivity. While the presence of extra-framework Cs species does not result in any additional decarbonylation and hydrogenation activity, the elimination of the extra-framework Cs (by washing) decreases the basicity of the CsNaX and allows the generation of weak acid sites. This treatment also leads to less restricted zeolite cavities, resulting in higher yield of hexenes via formation of a cyclic intermediate and lower α -to-internal olefins ratio in the product. When the Cs cation is not present in the catalyst (i.e., NaX), the decarbonylation activity rapidly decreases and undesired products are obtained.

Acknowledgements

This work has been partially supported by the National Science Foundation EPSCOR (Grant 0814361), the Oklahoma Bioenergy Center, and the Department of Energy (Grant DE-FG36G088064), the Thailand Research Fund (TRF) under the Royal Golden Jubilee Ph.D. Program, the Center for Petroleum, Petrochemicals, and Advanced Materials (PPAM), and the Petrochemical and Environmental Catalysis Research Unit of the Ratchadepiseksompote Endowment, Chulalongkorn University.

References

- [1] K. Suwannakarn, E. Lotero, J.G. Goodwin Jr., C.Q. Lu, *J. Catal.* 255 (2008) 279–286.
- [2] Q. Shu, Z. Nawaz, J. Gao, Y. Liao, Q. Zhang, D. Wang, J. Wang, *Bioresour. Technol.* 101 (2010) 5374–5384.
- [3] M. Ramos, A. Casas, L. Rodríguez, R. Romero, A. Pérez, *Appl. Catal. A* 346 (2008) 79–85.
- [4] G. Knothe, *Fuel Process. Technol.* 86 (2005) 1059–1070.
- [5] M.M. Conceição, V.J. Fernandes Jr., A.S. Araújo, M.F. Farias, I.M.G. Santos, A.G. Souza, *Energy Fuels* 21 (2007) 1522–1527.
- [6] M. Snäre, I. Kubičkova, P. Mäki-Arvela, D. Chichova, K. Eränen, D.Y. Murzin, *Fuel* 87 (2008) 933–945.
- [7] O.I. Senol, E.M. Ryymin, T.R. Vilijava, A.O.I. Krause, *J. Mol. Catal. A* 268 (2007) 1–8.
- [8] L. Boda, G. Onyesták, H. Solt, F. Lónyi, J. Valyon, A. Thernesz, *Appl. Catal. A* 374 (2010) 158–169.
- [9] F.A. Twaiq, N.A.M. Zabidi, S. Bhatia, *Ind. Eng. Chem. Res.* 38 (1999) 3230–3237.
- [10] T.J. Benson, R. Hernandez, W.T. French, E.G. Alley, W.E. Holmes, *J. Mol. Catal. A* 303 (2009) 117–123.
- [11] J.D. Adjaye, N.N. Bakshi, *Fuel Process. Technol.* 45 (1995) 161–183.
- [12] T. Sooknoi, T. Danuthai, L.L. Lobban, R.G. Mallinson, D.E. Resasco, *J. Catal.* 258 (2008) 199–209.
- [13] T. Sooknoi, J. Dwyer, *J. Mol. Catal. A* 211 (2004) 155–164.
- [14] D.J. Parrillo, A.T. Adamo, G.T. Kokotailo, R.J. Gorte, *Appl. Catal.* 67 (1990) 107–118.
- [15] Y.F. Shepelev, I.K. Butikova, Y.I. Smolin, *Zeolites* 11 (1991) 287–292.
- [16] C.E.A. Kirschhock, B. Hunger, J. Marten, P.A. Jacobs, *J. Phys. Chem. B* 104 (2000) 439–448.
- [17] F.J. Lázaro, J.L. García, V. Schünemann, C. Butzlaff, A. Larrea, M.A. Zaluska-Kotur, *Phys. Rev. B* 53 (1996) 13934–13941.
- [18] J. Li, R.J. Davis, *J. Phys. Chem. B* 109 (2005) 7141–7148.
- [19] P. Concepción-Heydorn, C. Jia, D. Herein, N. Pfänder, H.G. Karge, F.C. Jentoft, *J. Mol. Catal. A* 162 (2000) 227–246.
- [20] J. Weitkamp, S. Ernst, M. Hunger, T. Röser, S. Huber, U.A. Schubert, P. Thomasson, H. Knözinger, *Stud. Surf. Sci. Catal.* 101 (1996) 731–740.
- [21] A. Borgna, J. Sepúlveda, S.I. Magni, C.R. Apesteguía, *Appl. Catal. A* 276 (2006) 207–215.
- [22] T.R. Krawietz, D.K. Murray, J.F. Haw, *J. Phys. Chem. A* 102 (1998) 8779–8785.
- [23] R.J. Davis, *J. Catal.* 216 (2003) 396–405.
- [24] A. Aboulayt, C. Binet, J.C. Lavalley, *J. Chem. Soc., Faraday Trans.* 91 (1995) 2913–2920.
- [25] T. Armaroli, E. Finocchio, G. Busca, S. Rossini, *Vib. Spectrosc.* 20 (1999) 85–94.
- [26] M. Hunger, W. Wang, *Adv. Catal.* 50 (2006) 149–225.
- [27] R. Schenkel, A. Jentys, S.F. Parker, J.A. Lercher, *J. Phys. Chem. B* 108 (2004) 7902–7910.
- [28] H. Vinek, J.A. Lercher, H. Noller, *J. Mol. Catal.* 30 (1985) 353–359.
- [29] N. Takahashi, H. Matsuo, M. Kobayashi, *J. Chem. Soc., Faraday Trans.* 180 (1984) 629–634.
- [30] T. Danuthai, S. Jongpatiwut, T. Rirksomboon, S. Osuwan, D.E. Resasco, *Appl. Catal. A* 361 (2009) 99–105.
- [31] T. Danuthai, S. Jongpatiwut, T. Rirksomboon, S. Osuwan, D.E. Resasco, *Catal. Lett.* 132 (2009) 197–204.
- [32] T.Q. Hoang, X. Zhu, T. Sooknoi, D.E. Resasco, R.G. Mallinson, *J. Catal.* 271 (2010) 201–208.
- [33] J. Engelhardt, J. Szanyi, J. Valyon, *J. Catal.* 107 (1987) 296–306.
- [34] W.S. Wieland, R.J. Davis, J.M. Garces, *J. Catal.* 173 (1998) 490–500.
- [35] P.E. Hathaway, M.E. Davis, *J. Catal.* 119 (1989) 497–507.
- [36] M.A. Peralta, T. Sooknoi, T. Danuthai, D.E. Resasco, *J. Mol. Catal. A* 312 (2009) 78–86.
- [37] M. Snäre, I. Kubičkova, P. Mäki-Arvela, K. Eränen, D.Y. Murzin, *Ind. Eng. Chem. Res.* 45 (2006) 5708–5715.
- [38] S. Lerstari, P. Mäki-Arvela, H. Bernas, O. Simakova, R. Sjöholm, J. Beltrami, G.Q. Max Lu, J. Myllyoja, I. Simakova, D.Y. Murzin, *Energy Fuels* 23 (2009) 3842–3845.
- [39] J.C. Gee, D.S. Prampin, *Appl. Catal. A* 360 (2009) 71–80.
- [40] G. Martra, S. Coluccia, P. Davit, E. Gianotti, L. Marchese, H. Tsuji, H. Hattori, *Res. Chem. Intermed.* 25 (1999) 77–93.